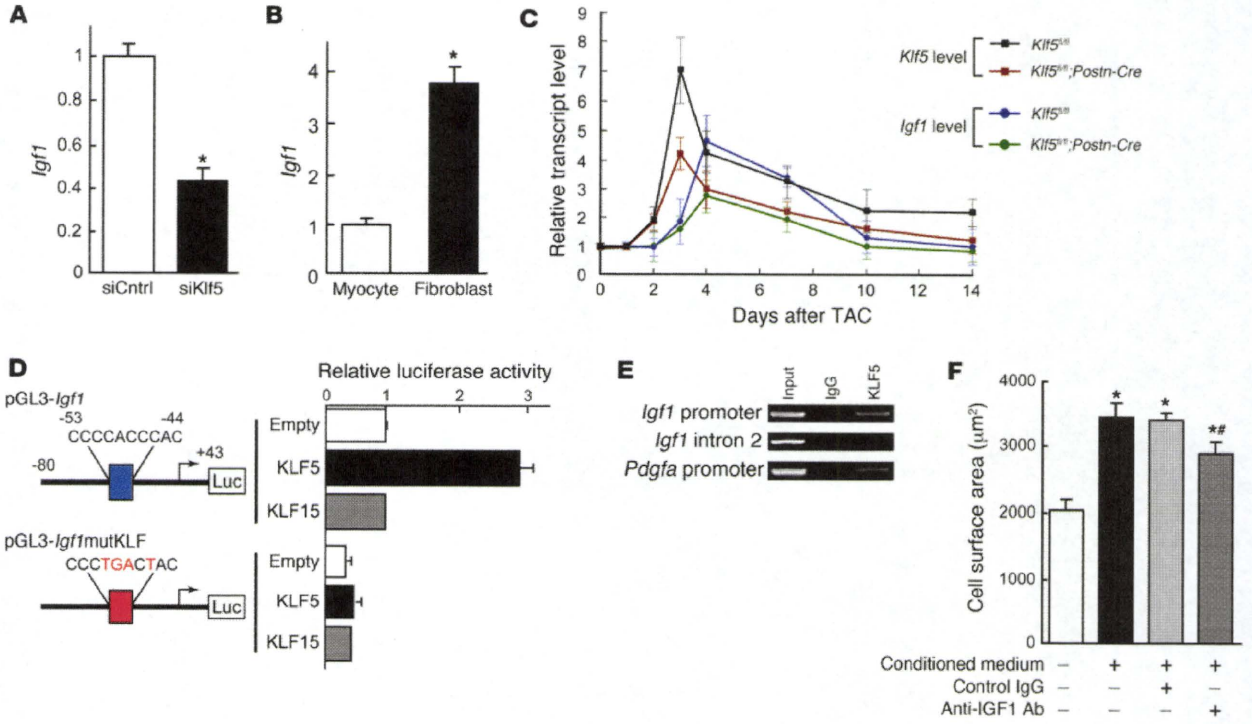

Figure 6

KLF5 transactivates the *Igf1* promoter. (**A**) KLF5 knockdown reduced *Igf1* expression in cardiac fibroblasts. KLF5 was knocked down as shown in Figure 5A. *$P < 0.01$ versus siCntrl. (**B**) Fibroblast-selective expression of *Igf1*. *Igf1* mRNA levels in cultured cardiac fibroblasts were normalized to those of 18s rRNA and then further normalized with respect to those in cardiomyocytes. *$P < 0.01$ versus cardiomyocytes. (**C**) Cardiac expression of *Klf5* and *Igf1* mRNA after LI-TAC in *Klf5*$^{fl/fl}$ and *Klf5*$^{fl/fl}$;*Postn-Cre* mice. Expression levels were normalized to those of 18s rRNA and then further normalized with respect to those in the hearts before TAC. (**D**) Reporter analysis of KLF5-depedent transactivation of the *Igf1* promoter. Luciferase reporter constructs driven by the wild-type *Igf1* promoter or a mutant promoter in which the potential KLF-binding site was mutated were cotransfected with either empty vector or a vector harboring *Klf5* or *Klf15*. Data are representative of 3 independent experiments. (**E**) ChIP assays of KLF5 binding to the *Igf1* and *Pdgfa* promoters. An intronic region of *Igf1* that does not contain a KLF-binding motif served as a negative control. (**F**) Effects of neutralizing IGF-1 on the cardiotrophic activity of fibroblast-conditioned medium. An antibody against IGF-1 (30 μg/ml) or normal IgG was added to the conditioned medium, after which the effect of the medium on cardiomyocyte surface area was analyzed. *$P < 0.01$ versus cells treated with SFM; #$P < 0.01$ versus cells treated with fibroblast-conditioned medium.

of transgenic overexpression of IGF-1 and IGF-1 receptor in cardiomyocytes, which were also suggestive of IGF-1's role in physiological hypertrophy and cardiac protection (42–46). Thus IGF-1 produced locally by fibroblasts appears to be a key mediator of cardiac hypertrophy and myocardial protection against pressure overload.

The present study identified *Igf1* as the target of KLF5 in fibroblasts involved in the cardiac adaptive response. However, KLF5 also likely controls the expression of genes other than *Igf1* and *Pdgfa*, including those encoding paracrine factors involved in regulating fibroblast function (Supplemental Table 1). We would therefore expect future studies of the gene networks controlled by KLF5 in cardiac fibroblasts to shed additional light on their homeostatic and pathological functions. In that regard, it will also be important to analyze the possible interplay between KLF5 and other members of the KLF family. Previous studies have demonstrated the functional roles played by several KLFs in the heart (34, 35, 47, 48). For instance, KLF15 negatively regulates cardiac fibrosis (34). It is therefore conceivable that networks of KLFs contribute to the myocardial responses to stress. Finally, our results suggest that therapeutic modulation of cardiac fibroblast function may represent a novel approach to the prevention and/or treatment of heart failure.

Methods

For experimental procedures not described herein, see Supplemental Methods.

Animals. Mice were housed in temperature-controlled rooms with a 12-hour light/12-hour dark cycle. All experiments were approved by the University of Tokyo Ethics Committee for Animal Experiments and strictly adhered to the guidelines for animal experiments of the University of Tokyo.

Generation of Klf5-floxed mice. A 12-kb *Klf5* fragment containing exons 1–3 was used to construct the targeting vector. The scheme for construction of the targeting vectors is shown in Supplemental Figure 5. The targeting construct was introduced into ES cells by electroporation, and G418-resistant clones were then examined for homologous recombination using Southern blot analysis with appropriate 3′ probes. Six ES clones that contained the correctly targeted *Klf5* locus were obtained, and 2 were injected into 129/Sv blastocysts to obtain chimeric mice. Male chimeras were bred with female transgenic mice expressing the enhanced site-specific recombinase FLP to remove the FRT-flanked neomycin cassette to generate heterozygous floxed *Klf5* (*Klf5*$^{fl/+}$) mice. *Klf5*$^{fl/+}$ mice were then backcrossed with C57BL/6 mice using the marker-assisted speed congenic method (49). The mice were genotyped by Southern blot analysis or PCR. Southern blot analysis was performed after *Hind*III digestion using a 396-bp PCR-amplified

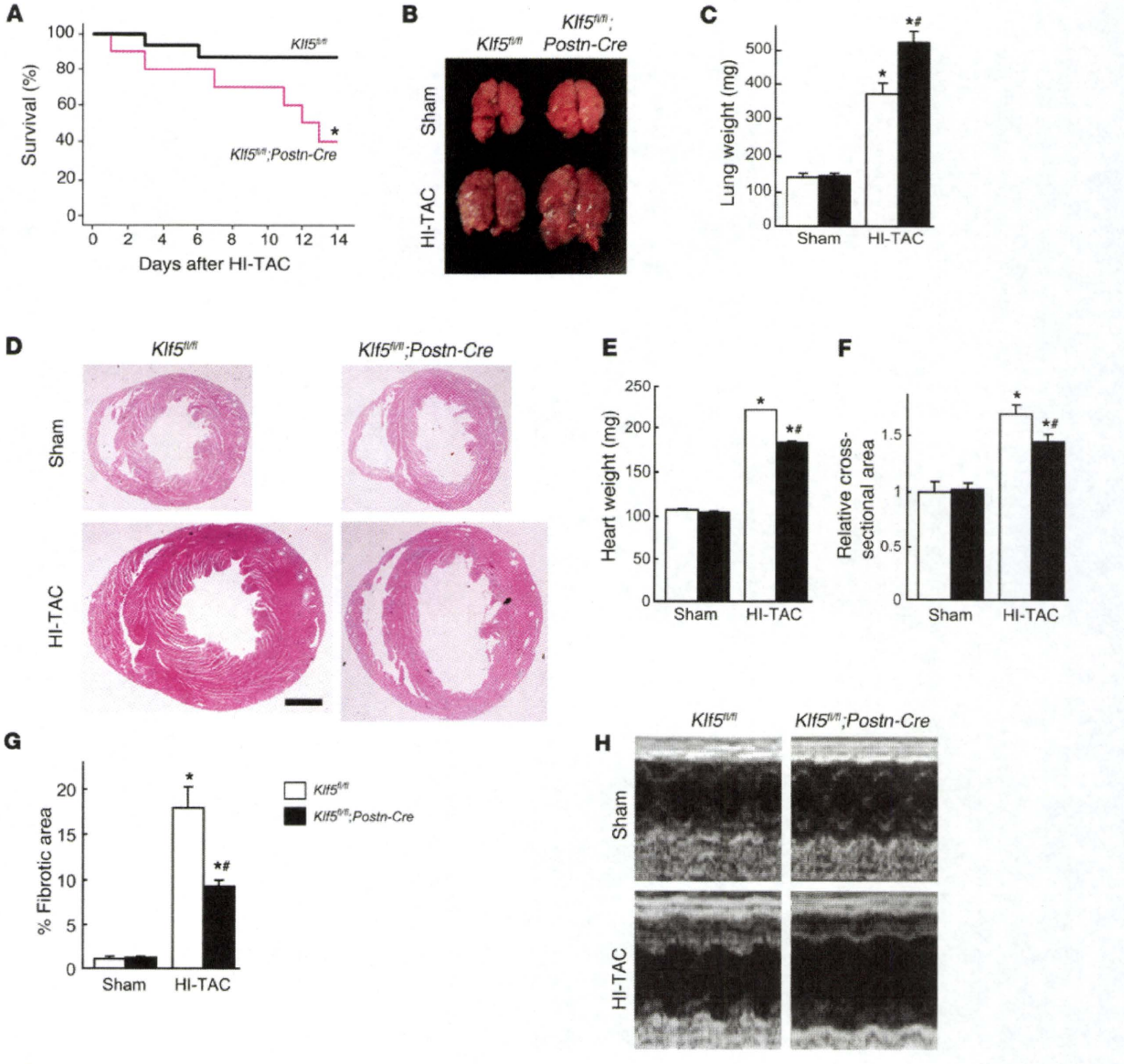

Figure 7

Cardiac fibroblasts are essential for the protective response elicited by severe pressure overload. (**A–H**) *Klf5*$^{fl/fl}$ and *Klf5*$^{fl/fl}$*;Postn-Cre* mice were subjected to HI-TAC or sham operation. (**A**) Kaplan-Meier survival analysis of *Klf5*$^{fl/fl}$ (n = 16) and *Klf5*$^{fl/fl}$*;Postn-Cre* (n = 10) mice after HI-TAC. *P < 0.05 versus *Klf5*$^{fl/fl}$. (**B**) Representative pictures of lungs 2 weeks after the operations. Note the severe lung edema in *Klf5*$^{fl/fl}$*;Postn-Cre* mice subjected to HI-TAC. (**C**) Lung weights in *Klf5*$^{fl/fl}$ (n = 5) and *Klf5*$^{fl/fl}$*;Postn-Cre* (n = 3) mice 2 weeks after the operations. (**D**) Representative low-magnification views of H&E-stained heart sections 2 weeks after the operations. Scale bar: 1 mm. (**E–G**) Heart weight/body weight ratios (**E**), relative cross-sectional areas of cardiomyocytes (**F**), and fibrotic areas (**G**) in *Klf5*$^{fl/fl}$ (n = 5) and *Klf5*$^{fl/fl}$*;Postn-Cre* (n = 3) mice 2 weeks after the HI-TAC operation. *P < 0.01 versus sham control of the same genotype; #P < 0.05 versus *Klf5*$^{fl/fl}$ mice subjected to HI-TAC. (**H**) M-mode echocardiographic tracings obtained 2 weeks after the operations.

probe for hybridization (Supplemental Figure 5). The probe for intron 1 was made by PCR using primers 5′-TGTCGTGGTGCTTTGAGAAG-3′ and 5′-TATCTTCCAGGCCCTGATTG-3′. PCR for genotyping was performed with primers A (5′-GCATCAGGAGGGTTTCATGT-3′) and B (5′-GTCTCGGCCTCATTGCTAAG-3′), which yielded 164-bp and 331-bp products for wild-type and floxed *Klf5* alleles, respectively.

Quantification of Cre-mediated recombination. Competitive PCR was performed to calculate the relative deletion frequency using primers A, B, and C (5′-TGACCCATTACCGAATCTACTG-3′), which produced 331-bp and 250-bp bands for the floxed and floxed-out *Klf5* alleles, respectively. The respective abundances of the floxed and floxed-out *Klf5* alleles were analyzed using real-time PCR with the same primer sets. To calculate absolute numbers of alleles in a given cell sample, we used external standards containing known numbers of DNA fragments derived from *Klf5*-floxed and floxed-out alleles.

TAC model. TAC was performed as described previously (50). Briefly, mice (8–10 weeks old, 21–24 g body weight) were anesthetized by intraperitoneal injection of a mixture of xylazine (5 mg/kg) and ketamine (100 mg/kg).

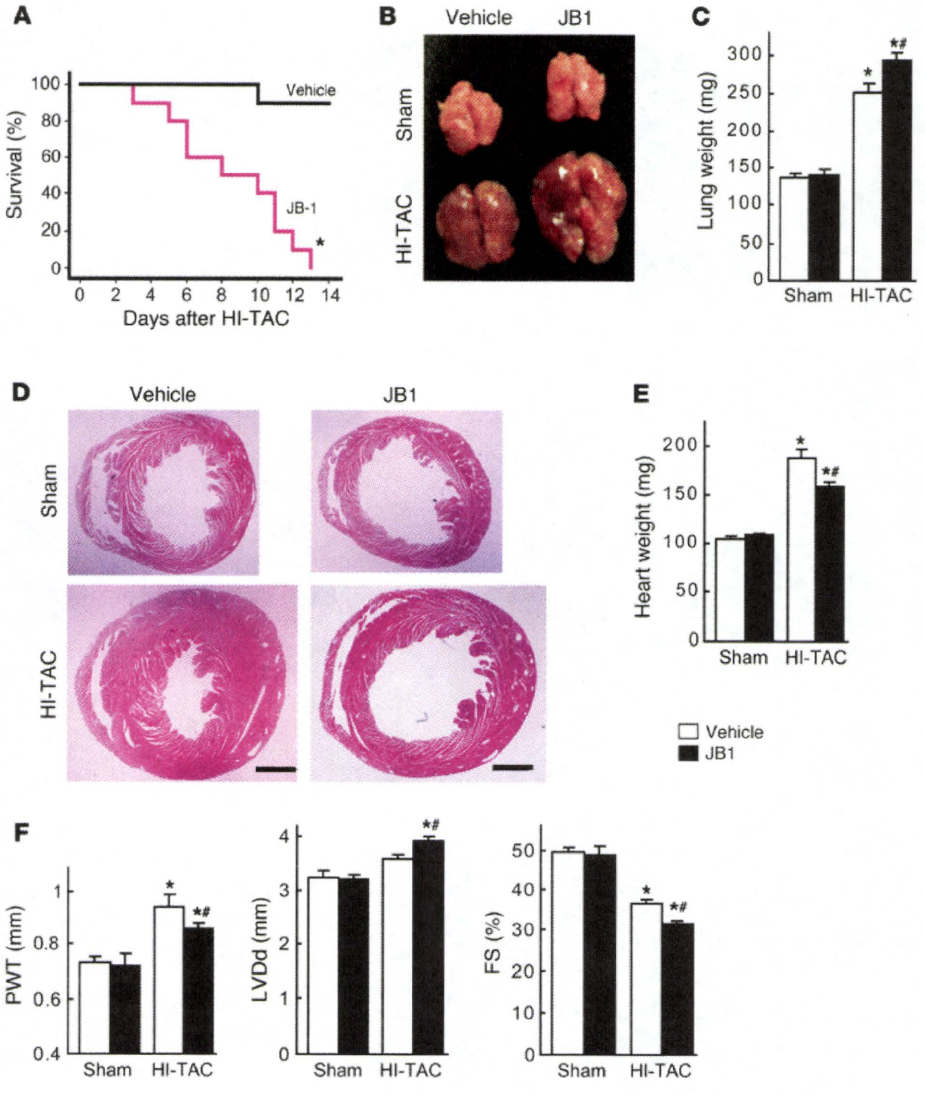

Figure 8
An IGF-1 receptor antagonist aggravates heart failure induced by severe pressure overload. (**A**) Kaplan-Meier survival analysis of wild-type mice treated with vehicle or JB1, a peptide IGF-1 receptor antagonist, after HI-TAC. $n = 10$ in each group. $^*P < 0.001$ versus vehicle. (**B**) Representative photographs of lungs taken 1 week after the operations. Note the severe lung edema in JB1-treated mice subjected to HI-TAC. (**C**) Lung weights in vehicle-treated and JB1-treated groups 1 week after the operations. $n = 5$ in each group. (**D**) Representative low-magnification views of H&E-stained heart sections 1 week after the operations. Scale bars: 1 mm. (**E**) Heart weights. (**F**) Echocardiographic analysis carried out 1 week after the operation. $^*P < 0.05$ versus sham controls in the same treatment group; $^\#P < 0.05$ versus vehicle controls subjected to HI-TAC.

The animals were then placed in a supine position, an endotracheal tube was inserted, and the animals were ventilated using a volume-cycled rodent ventilator with a tidal volume of 0.4 ml room air and a respiratory rate of 110 breaths/minute. The chest cavity was exposed by cutting open the proximal portion of the sternum. After the aortic arch between the innominate and left common carotid arteries was isolated, it was constricted with a 7-0 nylon suture tied firmly 3 times against a 25- or 27-gauge blunted needle for LI- and HI-TAC, respectively. Sham-operated mice underwent the identical surgical procedure, including isolation of the aorta, but without placement of the suture.

Administration of JB1, a peptide IGF-1 receptor antagonist. C57BL/6 mice (8–10 weeks old, 21–24 g body weight) were anesthetized by intraperitoneal injection of pentobarbital sodium (50 mg/kg). An incision was made in the midscapular region under sterile conditions, and an osmotic minipump (Alzet) containing either JB1 (BACHEM) dissolved in 0.15 mol/l NaCl and 1 mmol/l acetic acid or vehicle only was implanted. The delivery rate was 1 mg/kg/d for 14 days.

Echocardiography. Animals were lightly anesthetized with 2,2,2-tribromoethanol (200 mg/kg) and set in a supine position. Two dimensional (2D) guided M-mode echocardiography was performed using an echocardiogram (model 4500, Sonos) equipped with a 15 to 6 L MHz transducer (Philips). The heart at the level of the LV papillary muscle was imaged in the 2D mode in the parasternal short-axis view with a depth setting of 2 cm. LV diastolic posterior wall thickness (PWT), LV diastolic dimensions (LVDd), and LV end-systolic dimensions (LVDs) were measured. LV fractional shortening (%FS) was calculated as (LVDd – LVDs)/LVDd × 100.

Histological analysis. Heart sections were prepared as described previously (14) and stained with H&E for overall morphology. Immunohistochemical staining of KLF5 was performed using an anti-KLF5 monoclonal antibody (KM1784). A biotin-conjugated goat anti-rat antibody, streptavidin-conjugated horseradish peroxidase (Dako), and 3,3′-diaminobenzidine (DAB) were used to visualize labeling. For double staining of KLF5 and αMHC, we also used anti-αMHC monoclonal antibody CMA19 (51). Simple Stain AP(M) (Nichirei) and an Alkaline Phosphatase Substrate Kit I (Vector) were used to visualize labeling. To quantify cardiac interstitial fibrosis, we stained sections with elastic picrosirius red, after which images were captured with a digital camera and analyzed using Photoshop (Adobe) and Scion Image.

β-*Galactosidase staining.* Heart tissues were fixed for 12 hours at 4°C in PBS containing 0.4% glutaraldehyde, 0.01% Na deoxycholate, 0.1% NP40, 0.1 M $MgCl_2$, and 5 mM EGTA; rinsed 3 times for 30 minutes in PBS; and

then incubated for 24 hours at 37°C in a staining solution [1 mM $MgCl_2$, 20 mM $K_3Fe(CN)_6$, 20 mM $K_4Fe(CN)_6$, 1 mg/ml X-gal in PBS]. LacZ-stained sections were counterstained with nuclear fast red for nuclei, biotin-conjugated isolectin B4 (Vector) for ECs, and elastic picrosirius red for fibrosis.

Cardiomyocyte cross-sectional area. Heart sections were deparaffinized, rehydrated, and incubated for 1 hour at room temperature with FITC-labeled wheat germ agglutinin (Sigma-Aldrich) to visualize myocyte membranes. Regions that included the circular shapes of capillaries were selected from the epicardial side of the LV free walls. The mean cross-sectional area of cardiomyocytes was determined for each mouse from 60 to 80 cells.

RNA extraction and real-time PCR. Heart tissues were stored in RNAlater RNA stabilization reagent (QIAGEN) at 4°C. Total RNA was extracted using an RNeasy Fibrous Tissue Mini Kit (QIAGEN). First-strand cDNA synthesis was performed with 1 μg of total RNA, random hexamers, and SuperScript III Reverse Transcriptase (Invitrogen). Real-time PCR was performed using a QuantiTect SYBR Green PCR kit (QIAGEN) in a LightCycler (Roche). The expression level of each gene was normalized to that of 18s rRNA, which served as an endogenous internal control. The sequences of the PCR primers are shown in Supplemental Table 2.

Isolation of neonatal and adult cardiomyocytes and non-myocytes. Neonatal ventricles from 1-day-old ICR mice were separated and minced in ice-cold balanced salt solution, as described previously with minor modifications (52). To isolate cardiac cells, the tissues were incubated in a balanced salt solution containing 0.2% collagenase type 2 (Worthington Biochemical) for 6 minutes at 37°C with agitation. The digestion buffer was replaced 7 times, at which point the tissues were completely digested. The dispersed cells were incubated in 10-cm culture dishes for 80 minutes to remove non-myocytes. The unattached viable cells, which were rich in cardiomyocytes, were cultured on gelatin-coated dishes at 37°C in DMEM supplemented with 10% FBS and 10 μM cytosine 1-β-D-arabinofuranoside (Ara C) to inhibit fibroblast proliferation. Using this protocol, we consistently obtained cell populations containing at least 90%–95% cardiomyocytes. Non-myocyte cells that attached to the dishes were cultured in DMEM supplemented with 10% FBS and allowed to grow to confluence, then they were trypsinized and passaged at1:3. This procedure yielded cell cultures that were almost exclusively fibroblasts by the first passage. Experiments were carried out after 2 or 3 passages.

Adult cardiomyocytes were isolated using the Langendorff perfusion method as previously described (27). For isolation of non-myocyte-enriched cells, hearts were dissected free of vessels and atria, washed in ice-cold modified Krebs-Henseleit bicarbonate (KHB) buffer (pH 7.2) (Sigma-Aldrich), and quickly cut into pieces. The heart pieces were incubated in 5 ml of digesting solution (0.25 mg/ml Liberase TH [Roche] and 10 mM HEPES in balanced salt solution containing calcium and magnesium) for 8 minutes at 37°C with vigorous stirring. The supernatant was then added to 10 ml of ice-cold KHB. Five milliliters of fresh digesting solution was added to the remaining tissue fragments, and the digestion and sampling steps were repeated until all the tissue was dissolved. The collected cells were filtered through 35-μm nylon mesh (BD Falcon) and then used for flow cytometry. Levels of *Myh6* mRNA expression were much lower in the isolated cell populations than in normal whole hearts, indicating that the cell populations obtained using the method described here were enriched in non-myocytes (Supplemental Figure 15). Flow cytometric analysis (Figure 3) showed that the cell populations contained large fractions of fibroblasts and ECs.

Flow cytometric analysis and sorting. Single cells were isolated from adult hearts and incubated with PE-conjugated anti-Thy1 antibody (eBioscience), FITC-conjugated anti-CD31 antibody (BD Biosciences), and allophycocyanin-conjugated CD3e antibody (eBioscience), after which they were analyzed and sorted using a FACSAria II (BD Biosciences) and FlowJo software.

For analysis of β-galactosidase expression and the sorting of $LacZ^+$ cells, a FluoReporter LacZ Flow Cytometry Kit (Molecular Probes, Invitrogen) was used according to the manufacturer's recommendations. Cells were stained with the fluorogenic β-galactosidase substrate fluorescein di-β-D-galactopyranoside (FDG).

Production of medium conditioned by cardiac fibroblasts. Cardiac fibroblasts were grown to subconfluency in 10-cm dishes. The medium was then replaced with fresh serum-free DMEM, and the cells were incubated for additional 48 hours. The medium was then collected as conditioned medium.

siRNA. siRNA for *Klf5* and control siRNA were purchased from Dharmacon. Using Lipofectamine RNAiMax (Invitrogen), the siRNA at a final concentration of 20 nM in 10 ml of culture medium was transfected into mouse cardiac fibroblasts plated in 10-cm culture dishes. siRNA-mediated knockdown of *Klf5* did not affect mRNA expression levels in KLF family members that reportedly function in the cardiovascular system (e.g., *Klf2*, *Klf4*, *Klf10*, *Klf13*, and *Klf15*) (Supplemental Figure 16).

Morphometric studies of cells. Neonatal cardiomyocytes cultured in 3.5-cm dishes were maintained in serum-free DMEM for 24 hours, after which the culture medium was replaced with either fresh serum-free DMEM or medium conditioned by cardiac fibroblasts. To analyze the effects of neutralizing IGF-1, either anti–IGF-1 neutralizing antibody (Millipore) or control IgG (Sigma-Aldrich) was then added, and the cells were cultured for an additional 24 hours. To analyze the effects of growth factors, cells were first cultured for 24 hours in serum-free DMEM. The medium was then replaced with serum-free DMEM containing vehicle, IGF-1 (Wako), or PDGF-A (R&D Systems), and the cells were cultured for an additional 24 hours. The cells were then fixed in 2% paraformaldehyde and permeabilized for 10 minutes with 0.5% Triton X-100 (Sigma-Aldrich) in PBS, after which they were incubated in PBS containing 1% bovine serum albumin for 10 minutes to block nonspecific staining. They were then incubated with anti–sarcomeric α-actinin antibody (Sigma-Aldrich), followed by treatment with an Alexa-conjugated secondary antibody. Cardiomyocyte size was determined by measuring the surface area of sarcomeric α-actinin–positive cells.

Enzyme-linked immunoassay. To analyze secretion of ANP, cardiomyocytes were cultured in the serum-free DMEM for 24 hours and then stimulated with fresh serum-DMEM or medium conditioned by cardiac fibroblasts for 48 hours. The concentration of ANP protein in the culture medium was measured using an enzyme-linked immunoassay kit (Phoenix Pharmaceuticals).

Analysis of expression of alternatively spliced Igf1 mRNA. IGF-1 is controlled by 2 distinct promoters associated with untranslated exons 1 and 2, which generate two types of mRNA, containing either exon 1 (class 1 mRNA) or exon 2 (class 2 mRNA) plus a common block of translated exons (53–55). Expression of the two transcripts is differentially regulated in different tissues and species and during development. We therefore determined which mRNA was the major transcript in mouse heart. The respective abundances of the two transcripts were analyzed using real-time PCR with primer sets that specifically amplified either the class 1 or class 2 mRNA. To calculate absolute numbers of transcripts in a given amount of total RNA, we used external standards containing known numbers of class 1 or 2 cDNA fragments. We found that class 2 transcripts were much more abundant in both cardiac fibroblasts and cardiomyocytes than class 1 transcripts, and also in hearts after LI-TAC (Supplemental Figure 17). We therefore analyzed expression of class 2 mRNA as the major *Igf1* transcript in the heart and cardiac fibroblasts (Figure 6, A–C). *Igf1* class 1 and class 2 cDNA fragments were amplified using a forward primer specific for each leader exon (exon 1, 5′-ATGGGGAAAATCAGCAGTC-3′; exon 2, 5′-CTGCCTGTGTAAACGACCCGG-3′) and a reverse primer (exon 3-4 junction, 5′-GGCTGCTTTTGTAGGCTTCAGTGG-3′) (56).

Igf1 promoter–luciferase constructs. Because the class 2 *Igf1* mRNA is much more abundantly expressed than class 1 mRNA in the heart, we analyzed

the promoter associated with exon 2 (33). A genomic fragment of the 5′-flanking region and a part of exon 2 (–80 to +43 bp) was obtained by PCR using mouse genomic DNA. The promoter fragment was then subcloned into a pGL3 basic luciferase reporter vector (Promega) to generate pGL3-*Igf1*. A mutation within the potential KLF-binding motif was introduced by PCR to generate pGL3-*igf1*mutKLF. NIH-3T3 cells grown to 60%–80% confluence were then transfected with the vectors, after which luciferase activities were measured and normalized to β-galactosidase activity. The *Klf5* expression vector was described previously (57). The *Klf15* expression vector was obtained by inserting the *Klf15* cDNA into pCAGMS (14).

ChIP. ChIP assays were performed as previously described (29, 58). Mouse cardiac fibroblasts were formalin fixed, and then chromatin samples were immunoprecipitated using anti-KLF5 mouse monoclonal antibody (KM3918) or control IgG antibody. PCR was performed with the following region-specific primers: for the mouse *Igf1* KLF5 site within the exon 2–associated promoter, 5′-ACCCAGGCTCAGAGCATACC-3′ and 5′-GGGTCGTTTACACAGCAGGT-3′; for intron 2 (an intronic region +750 bp from the translation initiation site that does not contain KLF-binding motifs; negative control), 5′-CCTTCACCGCTCTCTGAAAC-3′ and 5′-CATCAGGGCTTCATGGTTCT-3′; and for the *Pdgfa* KLF5 site, 5′-ATGTAGCTGCCTGCGTGAG-3′ and 5′-CGACAGGGAGGGGGTTATAG-3′.

Statistics. Data are shown as mean ± SEM. Paired data were evaluated using Student's *t* test. Comparisons between multiple groups were made using 1-way ANOVA followed by a post-hoc Bonferroni test. Survival rates among mice were analyzed using long-rank test. *P* values less than 0.05 were considered statistically significant.

Acknowledgments

We thank N. Yamanaka, Y. Xiao, A. Ono, M. Hayashi, and E. Magoshi for their excellent technical assistance. This study was supported by Grants-in-Aid for Scientific Research (to N. Takeda, I. Manabe, R. Nagai) and a grant for Translational Systems Biology and Medicine Initiative from the Ministry of Education, Culture, Sports, Science and Technology of Japan; a research grant from the National Institute of Biomedical Innovation (to R. Nagai); and a research grant from the Japan Science and Technology Institute (to I. Manabe). P. Snider is supported by NIH T32 HL079995 Training Grant in Vascular Biology and Medicine, and S.J. Conway is partially supported by the Riley Children's Foundation and the NIH.

Received for publication June 24, 2009, and accepted in revised form October 21, 2009.

Address correspondence to: Ryozo Nagai or Ichiro Manabe, Department of Cardiovascular Medicine, University of Tokyo Graduate School of Medicine, 7-3-1 Hongo, Bunkyo, Tokyo 113-8655, Japan. Phone: 81-3-5800-6526; Fax: 81-3-3818-6673; E-mail: nagai-tky@umin.ac.jp (R. Nagai); manabe-tky@umin.ac.jp (I. Manabe).

1. Frey N, Olson EN. Cardiac hypertrophy: the good, the bad, and the ugly. *Annu Rev Physiol.* 2003;65:45–79.
2. Baudino TA, Carver W, Giles W, Borg TK. Cardiac fibroblasts: friend or foe? *Am J Physiol Heart Circ Physiol.* 2006;291(3):H1015–H1026.
3. Manabe I, Shindo T, Nagai R. Gene expression in fibroblasts and fibrosis: involvement in cardiac hypertrophy. *Circ Res.* 2002;91(12):1103–1113.
4. Eghbali M, et al. Collagen chain mRNAs in isolated heart cells from young and adult rats. *J Mol Cell Cardiol.* 1988;20(3):267–276.
5. Zak R. Cell proliferation during cardiac growth. *Am J Cardiol.* 1973;31(2):211–219.
6. Kuwahara K, et al. Involvement of cardiotrophin-1 in cardiac myocyte-nonmyocyte interactions during hypertrophy of rat cardiac myocytes in vitro. *Circulation.* 1999;100(10):1116–1124.
7. Harada M, et al. Significance of ventricular myocytes and nonmyocytes interaction during cardiocyte hypertrophy: evidence for endothelin-1 as a paracrine hypertrophic factor from cardiac nonmyocytes. *Circulation.* 1997;96(10):3737–3744.
8. Sano M, et al. Interleukin-6 family of cytokines mediate angiotensin II-induced cardiac hypertrophy in rodent cardiomyocytes. *J Biol Chem.* 2000;275(38):29717–29723.
9. Oka T, et al. Genetic manipulation of periostin expression reveals a role in cardiac hypertrophy and ventricular remodeling. *Circ Res.* 2007;101(3):313–321.
10. King KL, et al. Phenylephrine, endothelin, prostaglandin F2alpha' and leukemia inhibitory factor induce different cardiac hypertrophy phenotypes in vitro. *Endocrine.* 1998;9(1):45–55.
11. Ieda M, et al. Cardiac fibroblasts regulate myocardial proliferation through beta1 integrin signaling. *Dev Cell.* 2009;16(2):233–244.
12. Thum T, et al. MicroRNA-21 contributes to myocardial disease by stimulating MAP kinase signalling in fibroblasts. *Nature.* 2008;456(7224):980–984.
13. Haldar SM, Ibrahim OA, Jain MK. Kruppel-like Factors (KLFs) in muscle biology. *J Mol Cell Cardiol.* 2007;43(1):1–10.
14. Shindo T, et al. Kruppel-like zinc-finger transcription factor KLF5/BTEB2 is a target for angiotensin II signaling and an essential regulator of cardiovascular remodeling. *Nat Med.* 2002;8(8):856–863.
15. Nagai R, Suzuki T, Aizawa K, Shindo T, Manabe I. Significance of the transcription factor KLF5 in cardiovascular remodeling. *J Thromb Haemost.* 2005;3(8):1569–1576.
16. Forsberg K, Valyi-Nagy I, Heldin CH, Herlyn M, Westermark B. Platelet-derived growth factor (PDGF) in oncogenesis: development of a vascular connective tissue stroma in xenotransplanted human melanoma producing PDGF-BB. *Proc Natl Acad Sci U S A.* 1993;90(2):393–397.
17. Lindahl P, Johansson BR, Leveen P, Betsholtz C. Pericyte loss and microaneurysm formation in PDGF-B-deficient mice. *Science.* 1997;277(5323):242–245.
18. Raines EW. PDGF and cardiovascular disease. *Cytokine Growth Factor Rev.* 2004;15(4):237–254.
19. Andrae J, Gallini R, Betsholtz C. Role of platelet-derived growth factors in physiology and medicine. *Genes Dev.* 2008;22(10):1276–1312.
20. Agah R, et al. Gene recombination in postmitotic cells. Targeted expression of Cre recombinase provokes cardiac-restricted, site-specific rearrangement in adult ventricular muscle in vivo. *J Clin Invest.* 1997;100(1):169–179.
21. Lindsley A, et al. Identification and characterization of a novel Schwann and outflow tract endocardial cushion lineage-restricted periostin enhancer. *Dev Biol.* 2007;307(2):340–355.
22. Joseph NM, et al. The loss of Nf1 transiently promotes self-renewal but not tumorigenesis by neural crest stem cells. *Cancer Cell.* 2008;13(2):129–140.
23. Conway SJ, Molkentin JD. Periostin as a Heterofunctional Regulator of Cardiac Development and Disease. *Current Genomics.* 2008;9(8):548–555.
24. Snider P, et al. Periostin is required for maturation and extracellular matrix stabilization of noncardiomyocyte lineages of the heart. *Circ Res.* 2008;102(7):752–760.
25. Dorn GW, 2nd. Periostin and myocardial repair, regeneration, and recovery. *N Engl J Med.* 2007;357(15):1552–1554.
26. Soriano P. Generalized lacZ expression with the ROSA26 Cre reporter strain. *Nat Genet.* 1999;21(1):70–71.
27. Shioya T. A simple technique for isolating healthy heart cells from mouse models. *J Physiol Sci.* 2007;57(6):327–335.
28. Hudon-David F, Bouzeghrane F, Couture P, Thibault G. Thy-1 expression by cardiac fibroblasts: lack of association with myofibroblast contractile markers. *J Mol Cell Cardiol.* 2007;42(5):991–1000.
29. Oishi Y, et al. SUMOylation of Kruppel-like transcription factor 5 acts as a molecular switch in transcriptional programs of lipid metabolism involving PPAR-delta. *Nat Med.* 2008;14(6):656–666.
30. Serose A, Salmon A, Fiszman MY, Fromes Y. Short-term treatment using insulin-like growth factor-1 (IGF-1) improves life expectancy of the delta-sarcoglycan deficient hamster. *J Gene Med.* 2006;8(8):1048–1055.
31. Abbas A, Grant PJ, Kearney MT. Role of IGF-1 in glucose regulation and cardiovascular disease. *Expert Rev Cardiovasc Ther.* 2008;6(8):1135–1149.
32. McMullen JR. Role of insulin-like growth factor 1 and phosphoinositide 3-kinase in a setting of heart disease. *Clin Exp Pharmacol Physiol.* 2008;35(3):349–354.
33. Wang X, Talamantez JL, Adamo ML. A CACCC box in the proximal exon 2 promoter of the rat insulin-like growth factor I gene is required for basal promoter activity. *Endocrinology.* 1998;139(3):1054–1066.
34. Wang B, et al. The Kruppel-like factor KLF15 inhibits connective tissue growth factor (CTGF) expression in cardiac fibroblasts. *J Mol Cell Cardiol.* 2008;45(2):193–197.
35. Fisch S, et al. Kruppel-like factor 15 is a regulator of cardiomyocyte hypertrophy. *Proc Natl Acad Sci U S A.* 2007;104(17):7074–7079.
36. Ema M, et al. Kruppel-like factor 5 is essential for blastocyst development and the normal self-renewal of mouse ESCs. *Cell Stem Cell.* 2008;3(5):555–567.
37. Parisi S, et al. Klf5 is involved in self-renewal of mouse embryonic stem cells. *J Cell Sci.* 2008;121(Pt 16):2629–2634.
38. Jiang J, et al. A core Klf circuitry regulates self-renewal of embryonic stem cells. *Nat Cell Biol.* 2008;10(3):353–360.
39. Aizawa K, et al. Regulation of platelet-derived growth factor-A chain by Kruppel-like factor 5: new pathway of cooperative activation with nuclear factor-kappaB. *J Biol Chem.* 2004;279(1):70–76.
40. Pietrzkowski Z, Wernicke D, Porcu P, Jameson BA, Baserga R. Inhibition of cellular proliferation by

peptide analogues of insulin-like growth factor 1. *Cancer Res.* 1992;52(23):6447–6451.
41. Sano M, et al. p53-induced inhibition of Hif-1 causes cardiac dysfunction during pressure overload. *Nature.* 2007;446(7134):444–448.
42. Welch S, et al. Cardiac-specific IGF-1 expression attenuates dilated cardiomyopathy in tropomodulin-overexpressing transgenic mice. *Circ Res.* 2002;90(6):641–648.
43. Li B, et al. Insulin-like growth factor-1 attenuates the detrimental impact of nonocclusive coronary artery constriction on the heart. *Circ Res.* 1999;84(9):1007–1019.
44. Kajstura J, et al. IGF-1 overexpression inhibits the development of diabetic cardiomyopathy and angiotensin II-mediated oxidative stress. *Diabetes.* 2001;50(6):1414–1424.
45. Li Q, et al. Overexpression of insulin-like growth factor-1 in mice protects from myocyte death after infarction, attenuating ventricular dilation, wall stress, and cardiac hypertrophy. *J Clin Invest.* 1997;100(8):1991–1999.
46. McMullen JR, et al. The insulin-like growth factor 1 receptor induces physiological heart growth via the phosphoinositide 3-kinase(p110alpha) pathway. *J Biol Chem.* 2004;279(6):4782–4793.
47. Lavallee G, et al. The Kruppel-like transcription factor KLF13 is a novel regulator of heart development. *EMBO J.* 2006;25(21):5201–5213.
48. Subramaniam M, Hawse JR, Johnsen SA, Spelsberg TC. Role of TIEG1 in biological processes and disease states. *J Cell Biochem.* 2007;102(3):539–548.
49. Wakeland E, Morel L, Achey K, Yui M, Longmate J. Speed congenics: a classic technique in the fast lane (relatively speaking). *Immunol Today.* 1997;18(10):472–477.
50. Rockman HA, et al. Segregation of atrial-specific and inducible expression of an atrial natriuretic factor transgene in an in vivo murine model of cardiac hypertrophy. *Proc Natl Acad Sci U S A.* 1991;88(18):8277–8281.
51. Komuro I, et al. Isolation and characterization of two isozymes of myosin heavy chain from canine atrium. *J Biol Chem.* 1986;261(10):4504–4509.
52. Komuro I, et al. Stretching cardiac myocytes stimulates protooncogene expression. *J Biol Chem.* 1990;265(7):3595–3598.
53. Lin WW, Oberbauer AM. Alternative splicing of insulin-like growth factor I mRNA is developmentally regulated in the rat and mouse with preferential exon 2 usage in the mouse. *Growth Horm IGF Res.* 1998;8(3):225–233.
54. Shemer J, Adamo ML, Roberts CT Jr, LeRoith, D. Tissue-specific transcription start site usage in the leader exons of the rat insulin-like growth factor-I gene: evidence for differential regulation in the developing kidney. *Endocrinology.* 1992; 131(6):2793–2799.
55. O'Sullivan DC, Szestak TA, Pell JM. Regulation of IGF-I mRNA by GH: putative functions for class 1 and 2 message. *Am J Physiol Endocrinol Metab.* 2002;283(2):E251–E258.
56. Ohtsuki T, Otsuki M, Murakami Y, Hirata K, Takeuchi S, Takahashi S. Alternative leader-exon usage in mouse IGF-I mRNA variants: class 1 and class 2 IGF-I mRNAs. *Zoolog Sci.* 2007;24(3):241–247.
57. Oishi Y, et al. Kruppel-like transcription factor KLF5 is a key regulator of adipocyte differentiation. *Cell Metab.* 2005;1(1):27–39.
58. Manabe I, Owens GK. CArG elements control smooth muscle subtype-specific expression of smooth muscle myosin in vivo. *J Clin Invest.* 2001;107(7):823–834.